

Received September 20, 2017, accepted October 21, 2017, date of publication October 24, 2017, date of current version November 14, 2017.

Digital Object Identifier 10.1109/ACCESS.2017.2766157

Massive MIMO Beamforming With Transmit Diversity for High Mobility Wireless Communications

XUHONG CHEN¹, JIAXUN LU¹, PINGYI FAN¹, (Senior Member, IEEE),
AND KHALED BEN LETAIEF², (Fellow, IEEE)

¹Tsinghua National Laboratory for Information Science and Technology, Department of Electronic Engineering, Tsinghua University, Beijing 100084, China

²ECE Department, HKUST, Hong Kong

Corresponding author: Pingyi Fan (fpy@mail.tsinghua.edu.cn)

This work was supported in part by the 973 Program under Project 2012CB316100(2) and in part by NSFC under Project 61171064 and Project 61321061.

ABSTRACT Providing stable and fast data transmission service is challenging in a high mobility wireless communication system, where massive multiple-input multiple-output (MIMO) beamforming is deemed as a potential solution. In the literature, the majority of previous works focused on how to optimize the beamforming scheme with traditional side information like perfect or imperfect channel state information (CSI) in non-mobile or low mobility scenarios. However, it is hard to either track the channel or obtain perfect CSI in the high mobility scenario without large online computation, because the wireless channel appears to be fast time varying and double-selective in the spatial-temporal domain. In this paper, by exploiting the special characters in the high mobility scenario, we introduce an applicable low-complexity beamforming scheme with transmit diversity in the high mobility scenario with the aid of location information. The beam is generated and selected mainly based on the location information, where the beam weight is optimized to maximize the total service that one BS can provide. Moreover, to guarantee a full diversity gain in this joint scheme, an optimal beam selection algorithm is proposed. Besides, to maximize the total service competence of one base station, a closed-form power allocation solution for the multi-user scenario is derived. To solve the potential inter-beam interference in massive MIMO system, a location-aided algorithm is proposed to eliminate the interference and maximize the mobile service of the whole train at the same time. Theoretical analysis and multiple simulation results show that our scheme approaches the theoretical performance bound of adaptive beamforming scheme but with much lower complexity.

INDEX TERMS High mobility, massive MIMO, beamforming scheme, diversity gain, low complexity.

I. INTRODUCTION

A. BACKGROUND INTRODUCTION

In future 5G wireless communication systems, high mobility adaption is one of the key features in multiple-input multiple-output orthogonal frequency-division multiplexing (MIMO-OFDM) systems [1], which makes beamforming and space-time block coding (STBC) [2], [3] potentially promising in improving spectrum efficiency and reducing interference [4]. Even for now, high mobility wireless communication is also under increasingly great actual demands that for example, the construction and operation of high speed railway (HSR) is dramatically booming throughout the world, which triggers huge high-reliable and data-rich wireless communication demands for diverse entertainments from long

distance passengers [5]. However, the conventional systems such as GSM-R which is used for signaling can support no more than 200 Kbps data rate [6] and other dedicated systems [7], [8] which can support no more than 4 Mbps. Even the LTE-R can barely meet the actual estimated transmission requirements which according to [5] is as high as 65 Mbps with bandwidth 10 MHz for a train with 16 carriages and 1000 seats. If the communication demands between vehicles are discovered, standards like LTE-V should be considered as well [9]. Therefore, several new schemes and technologies (see [10]–[13]) attempting to partially solve the aforementioned problem have been raised up.

According to the literature, there are several critical problems aroused by high mobility and its special communication

environment [14]. First, the estimated maximum Doppler shift could be 945 Hz when the velocity is at 486km/h and the carrier frequency is at 2.1 GHz [5]. The Doppler effect would trigger inter-channel interference (ICI) [15] and consequently degrades the performance of systems such as MIMO-OFDM [16]. Second, frequent handovers and group handovers could increase the drop-off probability, which leads to the degradation of the quality of service (QoS) [17], especially considering the service time of one base station (BS) is diminished by high mobility [18]. Therefore, diverse assessments can be introduced to evaluate the beamforming performance [19] considering practical issues. Third, high mobility would probably result in traversing multiple terrains that diverse typical wireless communication scenarios such as viaduct and tunnel could be encountered within a short time. Therefore, complex channel environment would bring up new problems in channel modelings and detections [20] and meanwhile jeopardize the whole process of channel detection [21] because the wireless channel appears to be fast-varying and double-selective fading. Besides, near the boundary region of one BS, since the received signal-to-noise ratio (SNR) is very low [22], accurate instant channel detection becomes arduous and even imperfect channel state information (CSI) is not easily attainable [23], which fundamentally questions the significance of instant channel detection in this scenario, especially when considering its high complexity for massive MIMO [24], [25]. Fourth, omnidirectional antenna will cause mutual interference between public wireless communication system and dedicated system for HSR [26]. Thus, a proper power allocation scheme [27] according to the spatial distribution of BS [28] is indispensable. To generalize it, the high mobility character challenges the conventional beamforming in the aspects of channel detection, tracking and scheduling when considering the complexity-performance tradeoff. Therefore, it is paramount to introduce new perspectives and methods to redesign the beamforming scheme according to the aforementioned problems, which has not been studied in the literature to the best of our knowledge.

B. RELATED WORK AND MOTIVATION

Previous researches mainly focused on diverse beamforming scheme designs and their performance developments in the low mobility scenario for massive or non-massive MIMO systems. In [29], it essentially proposed an elementary method on combing adaptive beamforming with space-time block coding (STBC). Later in [16], it put forward a scheme on joint orthogonal switched beam with STBC whose performance approaches the theoretical bound of adaptive beamforming with lower complexity. In the last decade, certain parts of previous works focused on the theoretical performance exploration with different side information and preconditions [30], [31], whereas multiple applications [32], [33] and implementations [34], [35] of diverse joint switched beam schemes had been raised up. Until recent years, several conventional beamforming schemes [36]–[38] had been

introduced into high mobility scenarios such as HSR, which according to the theoretical analysis, had an impressive performance improvements. However, none of them had considered to design a joint beamforming scheme for massive MIMO system in the high mobility scenario with comparatively low computational complexity.

As explained earlier, the conventional approach of beamforming scheme is not suitable for massive MIMO systems in high mobility scenarios. The channel tracking is impossible in the high mobility scenario because the channel coherent time is less than 1 ms according to the real-scenario estimation in [5], namely, the channel experiences fast fading. Even if accurate CSI could be available, the benefits achieved by conventional joint adaptive beamforming schemes could be possibly offset by the enormous cost for continuously instant channel detections and huge complexity encountered in eigenvalue decomposing (ED) operations. Besides, for massive MIMO system, pilot contamination and its elimination will also consume enormous resources, which degrades the overall performance considering limited transmission time for each BS. According to the analysis of previous study [27] in the high mobility scenario as illustrated in Fig. 1, the coverage of one BS is generally divided into three regions: degree-of-freedom (DoF) limited region, intermediate region and SNR-limited region. Traditional beamforming scheme is beneficial in DoF limited region and intermediate region. However, in the SNR-limited region, since the received SNR could be extremely low, the benefits from conventional approaches are not worthy for tiny improvements. However, it is favourable that if the tiny improvements could be attained without large efforts in the same region.

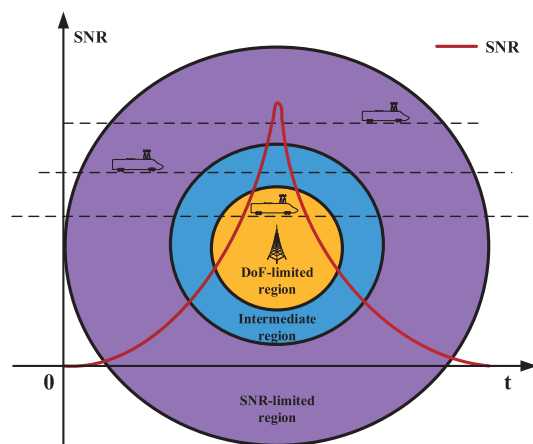


FIGURE 1. SNR fluctuation within one BS.

To the best of our knowledge, although high mobility arouses the aforementioned critical problems, it can also be beneficial in other perspectives that ground users with high mobility could be geographically predictable and usually move on fixed rail such as HSR or expressway, which means no spatial-random burst communication requests will occur and narrows down the coverage scope of the beamforming scheme. Therefore, the location information can be exploited

as a valuable side information and the real low-complexity beamforming scheme can be performed to compensate for the severe path loss in this scenario to a certain extent. Besides, the transmit diversity scheme like Alamouti STBC can function well in the absence of instant CSI and the large space for massive antenna installations on the top of the train can guarantee a full diversity gain in this joint scheme.

In this paper, we first take advantage of location information to design the low-complexity beamforming in the high mobility scenario for massive MIMO systems. In contrast to conventional joint adaptive beamforming or joint orthogonal switched beamforming, our beamforming scheme needs neither instantaneous channel detection nor large ED calculations of the estimated channel covariance matrix (CCM) to generate optimal beamforming weights and consequently, the large online computational complexity is reduced to a foreseeable extreme. The beamforming weights are pre-calculated and pre-stored at the BS according to the location of the train. When the train moves through one BS, the BS matches the train location information with stored beamforming excitation vector. To maximize the total service of one BS, we optimize the beam weight accordingly, where the optimal power allocation coefficient can also be pre-calculated and stored. Considering diversity gain is crucial to guarantee the overall performance in this scenario, an optimal beam selection algorithm is proposed and then, we maximize the total service in the multi-user scenario. For the practical issue, inter-beam interference is eliminated according to the location information based on the previous deductions. In the following discussions, three related fundamental problems will be investigated:

- *How does the proposed scheme solve the aforementioned critical problems in high mobility scenarios?*
- *How does the proposed scheme contribute in the aspect of bit-error rate (BER), successful handover probability and the total mobile service of one BS?*
- *How much is the performance gap between joint adaptive beamforming scheme and the proposed scheme?*

According to the results of numerical simulations, the proposed method is capable to perform beamforming with the aided of location information in a high mobility scenario like HSR, which alleviates the challenges in channel detections and diminishes the inherent large-online computational complexity. By properly designing directional beamforming scheme, significant improvement is observed in the aspects of BER, successful handover probability and total mobile service. Moreover, due to the exploitation of location information, the performance of the proposed location-aided beamforming scheme approaches the performance limit of the joint adaptive beamforming scheme.

The rest of this paper is organized as follows. Section II introduces the designed transceiver structure, the channel model and the evaluation methods for the high mobility scenario. Section III presents the detailed design of our location-aware massive MIMO beamforming scheme with optimal power allocation coefficient against large-scale fading.

In Section IV, we introduce the detailed full-diversity guarantee scheme and the optimal resource allocation scheme of beamforming for the multi-user scenario. In Section V, based on previous discussions, we provide a location-aided inter-beam interference elimination method for massive MIMO beamforming system. Section VI provides multiple simulation results justifying the analysis. Finally, we conclude it in Section VII.

Throughout the rest of the paper, matrices and vectors are denoted by bold capital and lowercase letters, respectively. Let $\mathbf{V} \in \mathbb{C}^{M \times N}$ mean that the complex matrix \mathbf{V} is consist of M rows and N columns. \mathbf{I}_N denotes an $N \times N$ identity matrix; $(\cdot)^T$ stands for transpose operation; $(\cdot)^*$ stands for complex conjugate operation; $(\cdot)^H$ stands for Hermitian transpose; \odot stands for the Hadamard product; $\|\cdot\|_F$ refers to the Frobenius norm and $\mathbb{E}(\cdot)$ to denote ensemble expectation.

II. SYSTEM MODEL

In this paper, we consider the downlink transmission of a massive multi-user MIMO system in the HSR scenario with K users and total N generated beams, where each carriage is deemed as a user in this scenario and is equipped with a single antenna. Aiming to solve the significant penetration loss (larger than 20 dB according to [6]) from the alloy carriages of high-speed trains, which raises the handoff failure rate per user link at the same time, a two-hop transmission structure for HSR is applied to achieve broadband transmission. The system is illustrated in Fig. 2 along with typical linear topology distribution of BS. The vertical distance between BS and the railway is denoted as d_0 and the approximate transmission coverage is denoted as R . Besides, the length of crossover coverage of adjacent BS denotes as d_c and the length of one carriage is denoted as d_n .

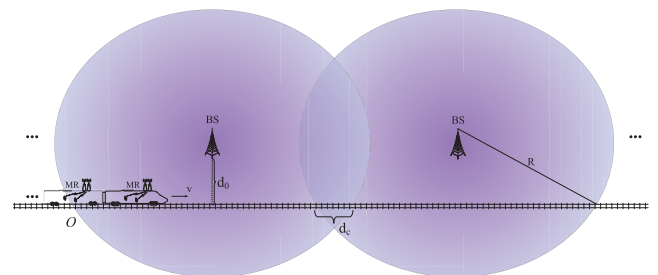


FIGURE 2. The two-hop structure and the linear topology of BS.

According to [37], Uniform Linear Array (ULA) antenna has proven its performance superiority in the HSR scenario and the multi-subarray structure is a good choice for beamforming [39] because the HSR itself can be treated as a distributed antenna system [40]. Therefore, our design for the downlink transmission is to equip the BS with multiple ULA subarray antennas. Each subarray has M -elements and communicates with different users. In the two-hop scheme, the mobile relay (MR) is mounted on the top of each carriage and user transmission inside will be forward to the BS through MR. Since MR and users are relatively static,

transmission between them can be settled by conventional approaches, such as WiFi. Therefore, the bottom neck of this two-hop scheme mainly falls into the hop between BS and MR. In this paper, we focus on the link between BS and the atop MR. Besides, since BS is deployed relatively far away from the rail, according to the characters of HSR scenarios, we consider far-field scattering characteristics, namely, the scatterers are far away from the BS¹ and therefore, the angular spread (AS) around the BS is relatively tight.

Since the total service time of one BS is short, we deem the train moves at a constant speed within one BS. For simplicity, The Doppler effect in this scenario will not be our primary consideration in our model. However, we can offset the inter-carrier interference (ICI) according to the method in [41] if it is required by the dedicated systems. The approximate channel coherent time according to the Doppler estimation in this scenario [5] is estimated to be no less than 10⁻³ second and thus we can adjust the block length of STBC accordingly.

A. CHANNEL MODEL

1) *Small-Scale Fading*: A high speed moving train may encounter diverse wireless communication scenarios in a comparatively short time such as mountainous terrain (channel fading obeys Rayleigh distribution), viaduct (channel fading obeys Rice distribution) and tunnel. Consequently, we consider to adopt Nakagami- \tilde{m} distribution to depict the envelop of received signals in rapid fading channel for its versatility [42] and better empirical data fitness [43]. The advantage of this model is that we can include more scenarios for the HSR scenario discussion. Besides, the \tilde{m} value of Nakagami- \tilde{m} fading channel in this HSR scenario can be obtained by prototype as in [44]. Accordingly, the fading channel can be expressed as

$$h(t) = A(t) \cdot e^{-j\phi_k}, \quad (1)$$

where $A(t)$ and $e^{-j\phi_k}$ denote its amplitude and phase, respectively. $A(t)$ is a Nakagami- \tilde{m} variable whose probability density function (pdf) is formulated as

$$p(A) = \frac{2A^{2\tilde{m}-1}}{\Gamma(\tilde{m})\Omega^{\tilde{m}}} \exp\left(-\frac{A^2}{\Omega}\right), \quad A \geq 0, \tilde{m} \geq 1/2 \quad (2)$$

where $\Gamma(\cdot)$ stands for the Gamma function and Ω represents the average power $\overline{A^2}$ such that $\Omega = \overline{A^2}/\tilde{m}$. The \tilde{m} represents the fading severity and the smaller the \tilde{m} is, the severer the channel fading will be. To be more specific, in case $\tilde{m} = 0.5$, the Nakagami- \tilde{m} fading reduces to one-sided Gaussian fading; in case $\tilde{m} = 1$, it degrades into Rayleigh fading; in case $\tilde{m} = (\mathcal{K} + 1)^2 / (2\mathcal{K} + 1)$, it is approximately equal to Rician fading with parameter \mathcal{K} ; in case \tilde{m} approaches infinity, it indicates no fading.

2) *Large-Scale Fading*: We adopt a normalized free-space path loss model in this scenario and we express it as a function of the distance $d(t)$ between the BS and the MR on the train:

¹This is especially suitable for viaduct and plain scenarios since the scatterers are located near around the receiver

$PL(d(t)) = d^\alpha(t)$. α is the path loss exponent and usually $\alpha \in [2, 5]$. And we set the time that the head of the train passes the point \mathbf{O} in Fig. 2 as $t = 0$ point such that $d(t)$ can be expressed as

$$d(t) = \sqrt{R^2 + (vt)^2 - 2Rvt\cos\beta + (h_{BS} - h_{tr})^2}, \quad (3)$$

where $\beta = \arccos \frac{d_0}{R}$, $t \in (0, t_m)$ and $t_m = \frac{d_s}{v}$. d_s represents the rail length covered by one BS and v stands for the velocity of the train. h_{BS} and h_{tr} denote the antenna height at the BS and train, respectively. Thus, the large scale fading can be equivalently expressed as

$$G(t) = \sqrt{1/PL(d(t))}. \quad (4)$$

B. TRANSCEIVER STRUCTURE

Assuming there are L subarrays, the baseband signal $S(t)$ is divided into L parallel substreams. The substream signals will be encoded in the STBC encoder as illustrated in Fig. 3. After that, each parallel output copies its encoded signal that guarantees the input signal onto the subarray possesses the same phase. The copied signals will be multiplied with a matched phase excitation $\theta_n \in \mathbb{C}^{M \times 1}$ ($n \in \mathcal{N} = \{1, 2, \dots, N\}$) and an accordingly amplitude excitation f_n for beamforming. The beamforming codebook is precalculated according to the BS coverage radius, distribution and train location information. The acquisition process of w_n will be later described in detail. A signal combiner performs a simple operation to obtain the ready-to-transmit vector signal for each subarray $x_l(t)$ ($l \in \mathcal{L} = \{1, 2, \dots, L\}$) which can be expressed as

$$x_l(t) = w_n^H \odot S_l(t), \quad (5)$$

where w_n is a $1 \times M$ vector selected from the beamforming codebook and $S_l(t)$ is a $M \times 1$ vector.

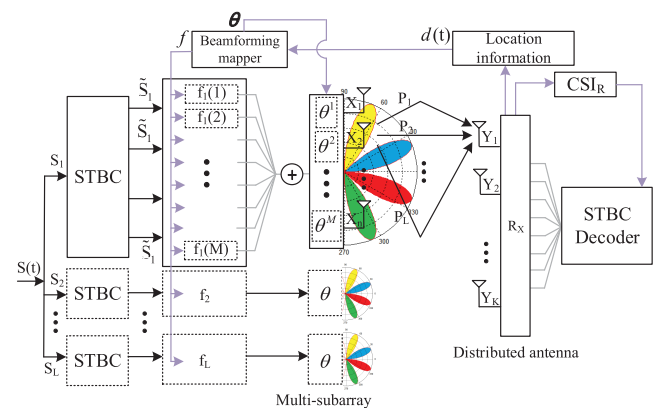


FIGURE 3. The transceiver structure of joint low-complexity beamforming scheme for massive MIMO HSR wireless communication systems.

C. EVALUATION METHODS

In the context, accurate train location information is assumed to be available by certain existed advanced techniques, such as Global Positioning System (GPS), Global Navigation

Satellite System (GNSS) system, accelerometer, goniometer, etc..

1) *Mobile Service*: Unlike conventional low-mobility users, users on a high speed train will not stay in the service range of one BS for a long time, where the train speed usually around 350 km/h and the service time is around 10 seconds according to different BS deployments. Consequently, the instantaneous capacity can not fully exhibit the service competence of one BS when applying massive MIMO beamforming. Therefore, based on the achievable rate, we define the mobile service to quantify the service competence as the integral of the instantaneous achievable rate $R(\tau)$ over a certain time period $[0, t_m]$

$$S = \int_0^{t_m} R(\tau) d\tau, \quad (6)$$

where t_m represents the total service time of one BS coverage.

2) *Successful Handover*: The handover performance is paramount in a HSR communication system because of short BS service time aroused by high mobility. Poor handover performance will trigger inferior QoS of time-sensitive service like voice and consequently, more data will be buffered for further transmission, which will probably cause traffic congestion. For the traditional handover trigger scheme, handover will be triggered when

$$\mathcal{P}_h(t) = \mathcal{P} \{ \xi_u(t) - \xi_v(t) \geq \varsigma, t \in [0, d_c/v], \quad (7)$$

where ξ_u and ξ_v stand for the received SNR from previous BS u and next BS v , respectively. ς stands for the trigger threshold. If the received signal is too weak to be decoded, an outage occurs

$$\mathcal{P}_o^i(t) = \mathcal{P} \{ \xi_i(t) < \eta \}, i = u, v, \quad (8)$$

where η stands for the outage threshold. Therefore, the handover succeed probability can be simply expressed as

$$\mathcal{P}_s(t) = \mathcal{P}_h(1 - \mathcal{P}_o^u(t))(1 - \mathcal{P}_o^v(t)). \quad (9)$$

III. LOW-COMPLEXITY LOCATION-AWARE BEAMFORMING SCHEME

In this section, we first describe the detailed criterions to generate appropriate beams, which includes phase excitation and amplitude excitation. After that, a general beam scheduling process for the HSR scenario is presented.

A. PHASE EXCITATION

According to the discussion in [45], directional transmission can be achieved with specific phase excitation into the antenna. Therefore, once the BS is deployed, the transmission coverage and relative position to one carriage are fixed, namely the directional transmission range of this scenario is determined. Because the AS is tight in the HSR scenario, the angle of arrival (AoA) of the strongest signal can be covered in a beam with appropriate beamwidth especially for the large distance transmission, where the beamwidth is the half power beamwidth according to [46]. Since we adopt multiple

single-array M -elements ULA, the total beam number N is determined on the appropriate AS and d_0 . If we simply take the Butler method as an example to generate the beam with $N = 2^c$ ($c \in \mathcal{N}^+$) total beams, the n -th beamforming weight can be expressed as

$$w_n = \sqrt{f_n} D_n(\beta_{lo}), \quad (10)$$

where $f_n = \sum_{m=1}^M f_n(m)$ ($m \in \mathcal{M}=\{1, 2, \dots, M\}$) denotes the power allocation coefficient for the n -th beam and $\sum_{n=1}^N f_n = 1$. $f_n(m)$ stands for the actual amplitude excitation on the m -th element and for a ULA antenna the amplitude excitation is defaulted to be equal on each element. $D_n(\beta_{lo})$ denotes the directivity of n -th beam with regard to the angle of departure (AoD) β_{lo} .

$$D_n(\beta_{lo}) = \frac{2(AF_n(\beta_{lo}))^2}{\int_0^\pi (AF_n(\phi))^2 \sin(\phi) d\phi}, \quad (11)$$

where

$$AF_n(\beta_{lo}) = \frac{\sin(0.5N\pi \cos(\beta_{lo}) - b_n\pi)}{0.5N\pi \cos(\beta_{lo}) - b_n\pi}, \quad (12)$$

and

$$b_n = -\frac{N+1}{2} + n, \quad (13)$$

$$\beta_{lo} = \arcsin\left(\frac{\sqrt{d_0^2 + (h_{BS} - h_{tr})^2}}{d(t)}\right). \quad (14)$$

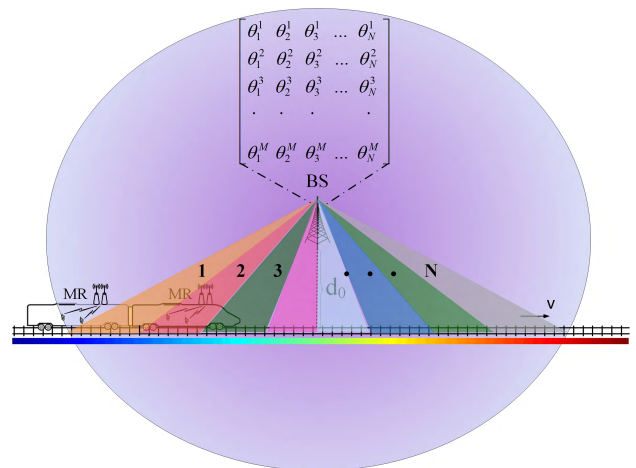


FIGURE 4. The sketch of massive MIMO beamforming for HSR wireless communication systems.

As illustrated in Fig. 4, once the BS is deployed, the beams directed to different locations are generated accordingly, namely, the BS can off-line calculate and pre-store the phase excitation θ_n of the n -th beam directed to a certain location, where $\theta_n = [\theta_n^1, \theta_n^2, \dots, \theta_n^m, \dots, \theta_n^M]^T$ and θ_n^m is the exact phase excitation on m -th element of the n -th beam. Consequently, the phase excitation mapper $\Theta \in \mathbb{C}^{M \times N}$ of each beam can be expressed as

$$\Theta = [\theta_1, \theta_2, \dots, \theta_N]. \quad (15)$$

Remark 1: According to the definition of directivity D , when the train moves toward BS, the directivity will increase; when the train leaves BS, the directivity will decrease; when $\beta_{lo} = \pi/2$, the directivity is maximized.

B. AMPLITUDE EXCITATION

As defined in Eq. (10), each beam possesses a power allocation coefficient f_n , where the constrained total transmit power \bar{P} at the BS is allocated to each beam according to this coefficient (i.e. $\bar{P} \cdot f_n$ represents the power allocated to beam n). After the power allocation process is done, the power can be divided as the amplitude excitation to each element. Since the instant CSI is not known at the BS and large-scale fading is dominant in this scenario (86.5% of Beijing-Shanghai HSR is viaduct scenario [47]), it is crucial to redesign resource allocation strategy in the HSR scenario according to the carriage location information $d(t)$ by transforming the conventional water-filling strategy into a location-aware water-filling against large-scale fading, where we adopt the channel capacity only subject to large-scale fading to evaluate the achievable transmission rate.

If we normalize the radiation efficiency of the antenna array, the achievable rate $R(t)$ of a single carriage at time $t, t \in (0, t_m)$ can be expressed as

$$R(t) = \sum_{n=1}^N \log\left(1 + \frac{\bar{P} \cdot f_n(t) \cdot D_n(t) \cdot G^2(t) \cdot h^2(t)}{\sigma_0^2}\right), \quad (16)$$

where \bar{P} represents the total power the BS can consumer at a certain time and $f_n(t)$ satisfies $\sum_{n=1}^N f_n(t) = 1$. σ_0^2 denotes the complex additive white Gaussian noise power. N represents the total generated beam number.

During the train traversing time, we assume the maximum selected beam number N_s for each carriage equals to 1 ($N_s = 1$). Under this assumption, to optimize the mobile service of single carriage (defined in Eq. (6)) over the whole time period equals to optimize the total data amount that can be transmitted in one BS. Consequently, the beamforming strategy with location-aware water-filling transforms into the maximization problem of mobile service, which can be formulated as

$$\begin{aligned} & \max_{f(t)} \quad S \\ & \text{s.t.} \quad \sum_{n=1}^N f_n(t) = 1, f_n(t) \geq 0. \end{aligned} \quad (17)$$

Note that $f_n = 0$ means no power is distributed to the n -th beam, that is, the n -th beam is not selected. The closed-form solution of this optimization problem is given in **Proposition 1**.

Proposition 1: Under the condition that transmit CSI is not known, the optimal power allocation coefficient satisfies

$$f_n(t) = \max \left\{ 0, \frac{1}{\lambda \bar{P}} - \frac{1}{\bar{P} D_n(t) \tilde{W}(t)} \right\} \quad (18)$$

and

$$\lambda = \frac{N_s}{\bar{P} + \sum_{n=1}^N \frac{1}{D_n(t) \tilde{W}(t)}}. \quad (19)$$

Proof: Proof of this proposition is given in appendix VII. ■

By observing this formula, the power allocation coefficient primarily depends on the selected beam number N_s , beam directivity $D_n(t)$ and $\tilde{W}(t)$. However, $D_n(t)$ and $\tilde{W}(t)$ is determined by the location of the train $d(t)$ and N_s has a maximum number. Consequently, it can be pre-calculated as well, where for n -th beam, the corresponding power allocation coefficient vector is f_n . Therefore, the whole amplitude excitation mapper of each beam can be expressed as

$$F = \begin{bmatrix} f_1(1) & f_2(1) & f_3(1) & \dots & f_N(1) \\ f_1(2) & f_2(2) & f_3(2) & \dots & f_N(2) \\ f_1(3) & f_2(3) & f_3(3) & \dots & f_N(3) \\ \vdots & \vdots & \vdots & \ddots & \vdots \\ f_1(M) & f_2(M) & f_3(M) & \dots & f_N(M) \end{bmatrix}. \quad (20)$$

Remark 2: Based on **Remark 1** and **Proposition 1**, the pre-set power allocation coefficient f_n for each beam increases when train moves toward to BS and decreases when train leaves BS; if $\beta_{lo} = \pi/2$, the power allocation coefficient is maximized.

C. THE LOCATION-AIDED BEAMFORMING PROCESS

According to the previous description, the total beamforming weight W of the location-aided beamforming can be expressed as

$$W = \Theta \odot F, \quad (21)$$

where the weight $w \in W$ is selected according to different location information.

When a carriage comes into the service range of one BS, the BS will choose the right n -th beam directed to the carriage location as illustrated in Fig. 5. Therefore, it is possible to obtain a phase excitation mapper Θ according to $d(t)$ and Θ is an $M \times N$ matrix, where N represents the total beam number and M represents the total element number. To be more specific, in Fig. 5 if the carriage is in the coverage of beam II, θ_2 will be found out from the pre-store excitation table and utilized. When it moves into the coverage of beam N, θ_N will be selected and applied. To generalize it, the conventional method by ED the CCM to acquire the optimal beamforming weights is replaced with a routing-similar scheme that the beamforming weight can be attained with searching the look-up table of phase excitation matrix with the aid of easy-to-get location information, which is compatible for the high mobility scenario such as HSR. The detailed procedure to initialize the phase excitation and beam scheduling are listed in **Algorithm 1**.

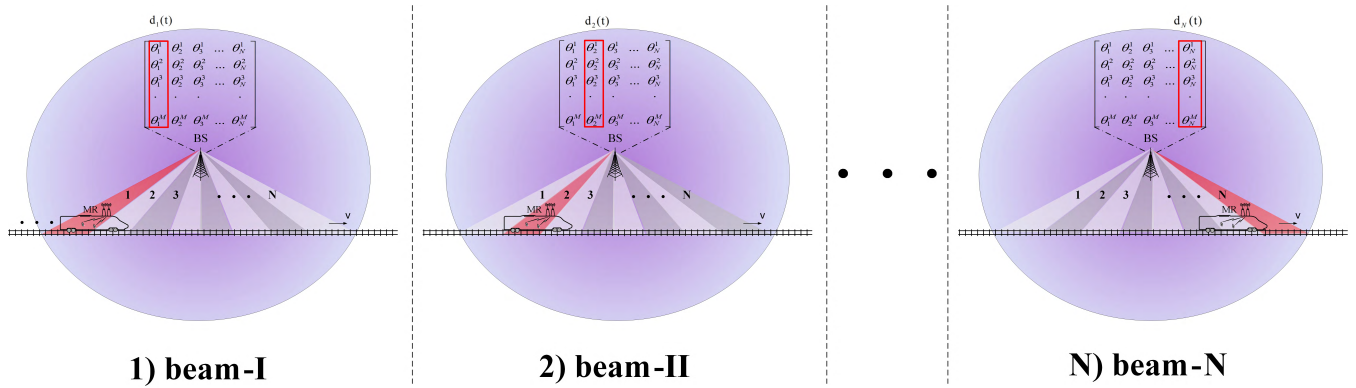


FIGURE 5. The beam activation process when a train goes through a BS.

Algorithm 1 The Excitation Acquisition and Scheduling Procedure

Require: $d(t)$.

Ensure: θ_n .

- 1: **Initialization:** $\theta_0 = []$, $d_0 = []$, BS stores Θ .
- 2: **Repeat:** BS is informed with train location information: $d_0 \leftarrow d(t)$.
- 3: BS matches the acquired $d(t)$ with Θ and finds the corresponding excitation: $\theta_0 \leftarrow \theta_n(d(t))$.
- 4: BS waits for the incoming next $d(t)$.
- 5: **Until:** $t > T_m$.
- 6: $\theta_0 \leftarrow \theta_1(d(t))$.

IV. MULTI-USER OPTIMAL BEAM SELECTION AND RESOURCE ALLOCATION

A. BEAMFORMING STRATEGY TO GUARANTEE DIVERSITY

If the carriage is in the effective coverage of one beam, it is paramount to guarantee the orthogonality of the chosen beam according to [48], because it is not the less-accurate directivity of the beam that degrades the system performance but the nonorthogonality of the strongest signals. Although the large space to deploy antenna on the top of the train will guarantee full diversity, it is also crucial to re-guarantee the full diversity from the beam selection process otherwise dramatic performance degradation will occur.

In the multi-user HSR scenario, the total number of the MR is usually fixed due to the restriction of maximum train length, which is much smaller than the number of beams that only some of the beams will be eventually selected for transmission. For most cases in this scenario, the strongest signal will be concentrated on only one or two beams because it is estimated that viaduct scenario occupies 80 percent of the entire HSR [5], which makes line-of-sight (LOS) signal strong and consequently, the large scale fading is dominant for most time compared with small scale fading, especially for the far-end of the BS coverage. If the beams with appropriate width are generated, the strongest signals are either in the same beam or from the adjacent two beams at most. We give an example of two adjacent users in Fig. 6.

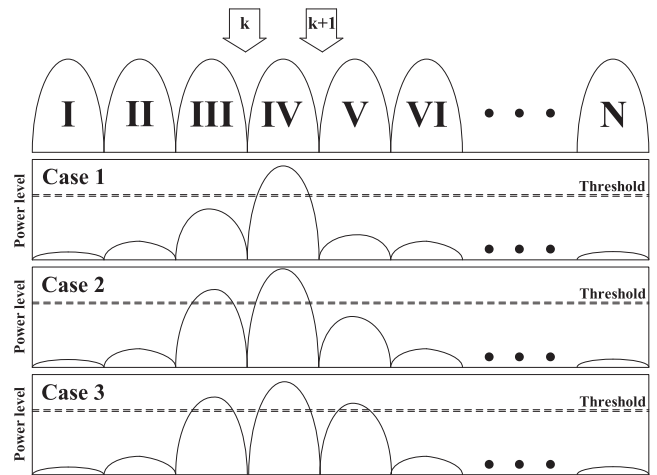


FIGURE 6. The beam selection process for three different cases.

Therefore, without loss of generality, three diverse selection cases with multipath signals are considered, where the power level is based on uplink measurements. For the first cases as illustrated in Fig. 6, there is only one dominant beam that the power level is stronger than the rest two beams. According to conventional beam selection scheme, if a threshold is not pre-introduced, the beam selection process merely select the strongest signal and then only beam IV be chosen. It is reasonable to conduct the selection process in case one. However, if case two or three emerges due the complex environment of HSR, this selection scheme fails to cover all the incoming paths, which inevitably leads to performance degradation due to signal correlation. Therefore, a new beam selection scheme is proposed for the HSR scenario to avoid the aforementioned situation.

In the designed scheme, a power window threshold is introduced to select the potential qualified beams, where the threshold is usually 3 dB less than the maximum power level. Therefore, all the qualified beams will be temporarily reserved for the potential selection process. For instance, in case two, beam III and IV will be reserved. However, to reduce correlation with respect to each other, if three beams are qualified and reserved, only the nonadjacent two beams

will be selected that in case three, beam III and V will be utilized for transmission. The detailed selection process is described as in **Algorithm 2**.

Algorithm 2 The Beam Selection Process for Diverse Cases

Require: $\theta_{n-1}, \theta_n, \theta_{n+1}$.

Ensure: $\theta_n; \theta_{n-1}, \theta_n; \theta_{n-1}, \theta_{n+1}$.

- 1: **Initialization:** power threshold Ψ , power level in qualified beam Ψ_n , selected beam $\theta_s = []$.
- 2: **if** $\Psi < \Psi_n, \Psi > \Psi_{n-1}, \Psi > \Psi_{n+1}$ **then**
- 3: $\theta_s \leftarrow \theta_n;$
- 4: **else if** $\Psi < \Psi_n, \Psi < \Psi_{n-1}, \Psi > \Psi_{n+1}$ **then**
- 5: $\theta_s \leftarrow \theta_n, \theta_{n-1};$
- 6: **else if** $\Psi < \Psi_n, \Psi < \Psi_{n-1}, \Psi < \Psi_{n+1}$ **then**
- 7: $\theta_s \leftarrow \theta_{n-1}, \theta_{n+1};$
- 8: **end if**
- 9: **return** θ_s .

This simple and indispensable selection process will not introduce much online computation because for most cases, only one beam is qualified as described before. Even for the remaining situations, only three beams will be temporarily reserved. Therefore, this algorithm possesses a favourable robustness. By applying this method, other non-LOS scenarios are considered and optimized.

B. MULTI-USER RESOURCE ALLOCATION FOR BEAMFORMING

After the appropriate beam is selected for each carriage, the resource allocation is paramount to maximize the total service competence. Based on the single carriage scenario, we consider the resource allocation for multiple carriages without inter-beam interference first, where only one beam is allocated to a single carriage. According to the aforementioned beamforming scheme, the received power of carriage k can be expressed as

$$P_k(t) = \sum_{n=1}^N i_{k,n} \bar{P} w_n(t) G_k^2(t) h_k^2(t), \quad (22)$$

where in order to avoid inter-beam interference, the selected beam number N_s for carriage k is one. $i_{k,n} \in \{0, 1\}$ stands for an index of beam selection, where $i_{k,n} = 1$ means beam n is selected for carriage k for transmission, otherwise $i_{k,n} = 0$. Consequently, the power allocated for user k ($p_{k,n}$) when beam n is selected ($i_{k,n} = 1$) can be expressed as: $p_{k,n}(t) = \bar{P} f_{k,n}(t)$. The corresponding normalized achievable rate for carriage k can be expressed as

$$R_k(t) = \log(1 + \gamma_k(t)), \quad (23)$$

where

$$\gamma_k(t) = \frac{P_k(t)}{\sigma_k^2(t)} \quad (24)$$

represents the MR received signal-to-noise ratio (SNR) and $\sigma_k^2(t)$ represents the power of additive white Gaussian noise at user k .

Based on the previous analyses, our resource allocation target is to maximize the total mobile service of the train with diverse power allocation coefficient $f_{k,n}$ to each beam, which can be expressed as

$$\max_{f_{k,n}} \sum_{k=1}^K S_k \quad (25)$$

$$s.t. \sum_{k=1}^K \sum_{n=1}^N f_{k,n}(t) = 1, f_{k,n}(t) \geq 0. \quad (26)$$

Note that $f_{k,n}(t) = 0$ means no power is distributed to the n -th beam, that is, the n -th beam is not selected for user k at system time t . The closed-form solution of this optimization problem is given in **Proposition 2**.

Proposition 2: Under the condition that transmit CSI is not known, the optimal power allocation coefficient satisfies

$$f_{k,n}(t) = \max \left\{ 0, \frac{1}{\lambda K \bar{P}} - \frac{1}{\bar{P} \sum_{n=1}^N i_{k,n} D_n(t) W_k(t)} \right\} \quad (27)$$

and

$$\lambda = \frac{1}{\bar{P} + \sum_{k=1}^K \frac{1}{\sum_{n=1}^N i_{k,n} D_n(t) W_k(t)}}. \quad (28)$$

Proof: Proof of this proposition is given in appendix VII. ■

V. INTER-BEAM INTERFERENCE ELIMINATION

Based on the previous discussion, we consider a much complicated situation that during the beam selection process, more than one beams are selected for a single carriage ($N_s > 1$), which may be treated as a beam combining process. However, this beam combination can trigger the inter-beam interference. The inter-beam interference is defined as one beam is utilized by multiple users, where for the most case in the HSR scenario, it stands for one beam is utilized by different carriages within the same BS. To be more specific, the inter-beam interference will occur with a large probability between adjacent carriages under this LOS scenario.

Therefore, during the beam selection process, the received power of carriage k can be expressed as

$$P_k(t) = \sum_{n=1}^N i_{k,n} \bar{P} w_n(t) G_k^2(t) h_k^2(t). \quad (29)$$

Consequently, the inter-beam interference for carriage k can be expressed by

$$I_k(t) = \sum_{j=1, j \neq k}^K \sum_{n=1}^N i_{j,n} \bar{P} w_n(t) G_j^2(t) h_j^2(t), \quad (30)$$

where $i_{j,n}$ stands for the index of interference beam and it subjects to $\sum_{j=1, j \neq k}^K \sum_{n=1}^N i_{j,n} \leq \sum_{n=1}^N i_{k,n}$.

Therefore, the achievable rate can be expressed as

$$R'_k(t) = \log(1 + \Gamma(t)), \quad (31)$$

where

$$\Gamma(t) = \frac{P_k(t)}{I_k + \sigma^2(t)} \quad (32)$$

represents the received signal-to-interference-plus-noise ratio (SINR).

The object here is to maximize the total mobile service of the whole train when considering the inter-beam interference for location-aided massive MIMO beamforming, which can be expressed as the following optimization problem.

$$\max_{i_{k,n}} \sum_{k=1}^K \int_0^{t_s} R'_k(\tau) d\tau \quad (33)$$

$$s.t. \sum_{j=1, j \neq k}^K \sum_{n=1}^N i_{j,n} \leq \sum_{n=1}^N i_{k,n}, i_{k,n} \in \{0, 1\} \quad (34)$$

Because the above optimization problem is non-convex, we aim to solve it with a sub-optimal location-aided searching-based algorithm instead of an optimal closed-form solution. For a high-speed train, even the carriage number of a train is limited, the computational complexity of full-search algorithm will probably leads to performance degradation in real-scenario application since massive MIMO is considered. Fortunately, according to the previous conclusions in **Remark 1**, **Remark 2** and **Proposition 2**, we find that the beam near the center of BS possesses a higher directivity and also occupies a larger power allocation coefficient due to the better channel condition, which inspires us to optimize the searching algorithm based on the train location again, namely, if two adjacent carriages select one or several common beams at the same time, the carriage near the BS has the priority to occupy a beam with higher gain.

Therefore, based on the aforementioned discussion, the location-aided beam-selection searching algorithm is given in **Algorithm 3**.

Algorithm 3 The Location-Aided Beam Selection Against Inter-Beam Interference

Initialization:

$$i_{k,n}, a[\cdot] = [d_1(t), d_2(t), \dots, d_K(t)].$$

1. **for** $k = 1$ to K **do**
2. $k^* = \arg \min_k d_k(t)$;
3. **for** $n = 1$ to N **do**
4. **if** $i_{k^*,n} = 1, k^* + 1 \leq K$ **then**
5. $n^* = n, i_{k^*+1,n} = 0$;
6. **else if** $i_{k^*,n} = 1, k^* - 1 \geq 1$ **then**
7. $i_{k^*-1,n} = 0$;
8. **end if**
9. **end for**
10. $a[k^*] = 0$;
11. **end for**

Therefore, the whole beam scheduling process to avoid inter-beam interference is based on the continuous feed back of train location information. For instance, during the time the

train traverses the BS coverage, before the phase excitations for the selected beams directed to each carriage are applied by the antenna, the carriage which is the closest to the BS (i.e. the 2nd carriage) will check whether the selected beams (i.e. the 7th and 8th beam) are also occupied by other carriages (i.e. the 1st or 3rd carriage). If occupied (the 1st carriage also select the 7th beam for transmission), other carriage will release the beams (7th beam) and re-select. After it, the second closest carriage will also perform the same operation until the last carriage is done.

VI. SIMULATION RESULTS AND DISCUSSIONS

In this section, several numerical results are presented. The main simulation parameters are illustrated in TABLE I and we assume an accurate Doppler shift compensation at the receiver as in [41]. We label the joint adaptive beamforming as STBC-ABF and our scheme as STBC-LBF respectively for concise expression hereinafter.

TABLE 1. Parameter settings.

R	d_c	v	h_{BS}	h_{tr}	N_T	N_R
1 km	0.4 km	360 km/h	25 m	3 m	16	2
α	G_c	Data length	η	Γ	M	d_n
3.03	1	10^6	3 dB	1 dB	32	25 m

A. BER AND HANDOVER

We first exhibit the BER performance along the rail since the large-scale fading is dominant. As illustrated in Fig. 7, three different cases are investigated as a comparison for a single carriage. The STBC-LBF scheme can improve the BER performance along the rail especially at the far-side of the BS with much lower complexity, which upgrades the QoS by enlarging the effective transmission ranges and benefits the handover process potentially. Moreover, even the theoretical STBC-ABF scheme owns the best performance, our STBC-LBF scheme possesses a tiny potential performance drop compared with STBC-ABF, which is acceptable since instant CSI is not exploited in our scheme. However,

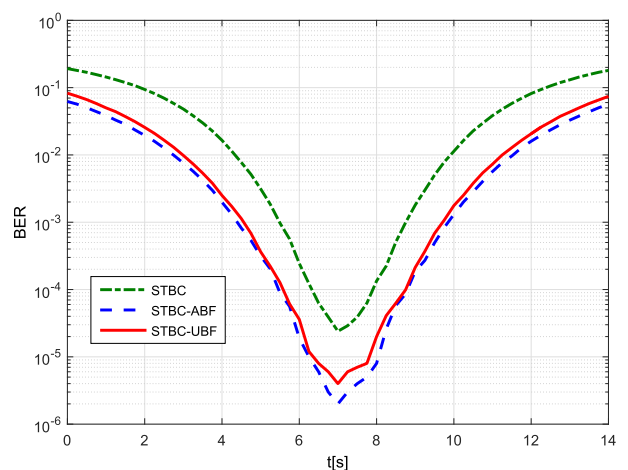


FIGURE 7. The BER performance along the rail, $d_0 = 100$ m.

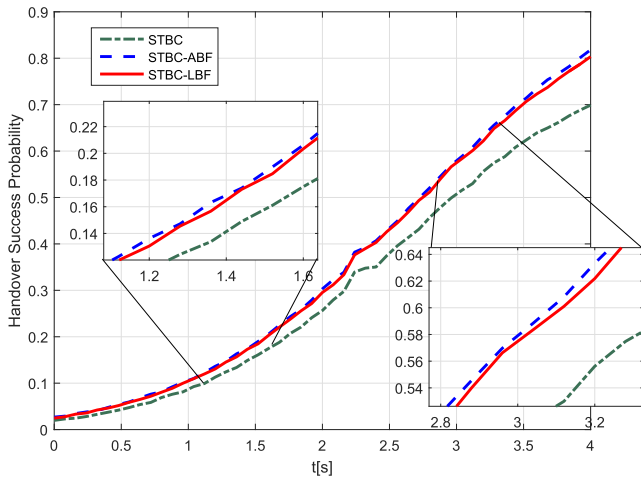


FIGURE 8. Handover succeed probability over diverse schemes, $d_0 = 100$ m.

from the practical perspective, the theoretical performance gain in STBC-ABF may be offset by the computation overhead and system complexity to implement ED considering the restrictions for the HSR scenario, which makes the STBC-LBF an optimal choice for the HSR scenario.

Then, as defined in Eq. (9), the handover succeed probability is exhibited in Fig. 8 since a large amount of handover will be triggered in the HSR scenario. We only evaluate the received SNR from one BS and the whole handover time is around 4 seconds. Again, the performance of STBC-LBF scheme approaches to STBC-ABF while it possesses a major improvement against STBC alone, which in another perspective, reduces the handover region and saves more time for data transmission. This improvement becomes more beneficial if the transmission coverage range of one BS is reduced through applying millimeter wave.

B. SINGLE CARRIAGE MOBILE SERVICE

More importantly, We conducted two pairs of simulations for single carriage mobile service with different transmit powers

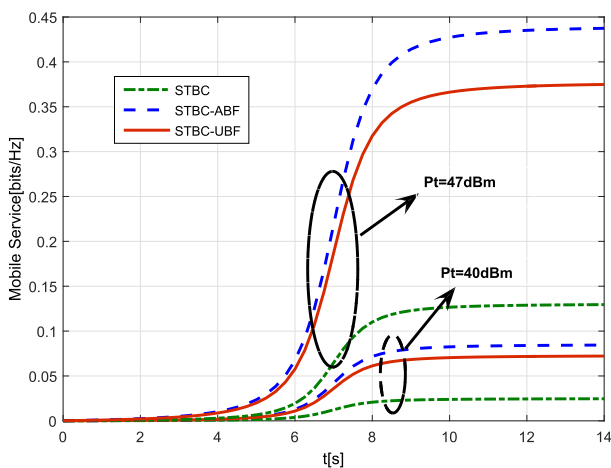


FIGURE 9. Mobile service comparison with diverse schemes, $d_0 = 100$ m.

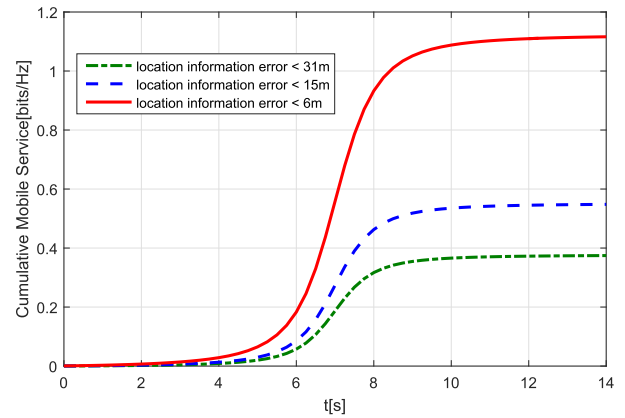


FIGURE 10. Mobile service comparison with different location information error, $d_0 = 100$ m.

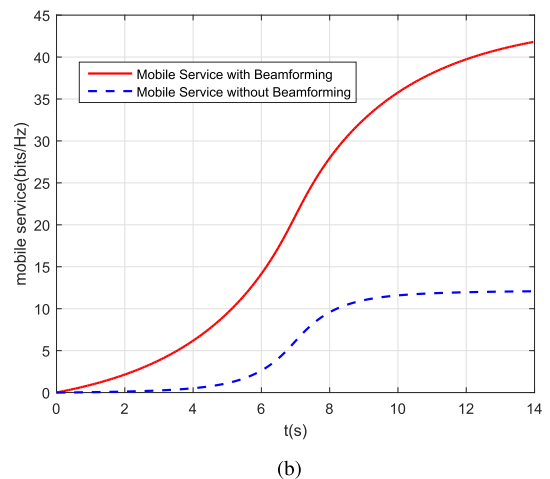
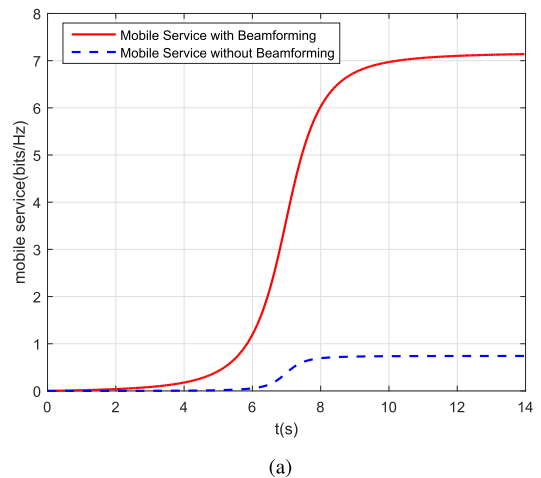


FIGURE 11. Mobile service comparison under different transmit power with/without beamforming, $d_0 = 50$ m. (a) 30dBm. (b) 40dBm.

as illustrated in Fig. 9. By applying the optimal beam selection algorithm, the total amount of data that can be transmitted within one BS is largely improved, where the STBC-LBF owns a nearly same performance as STBC-ABF scheme, especially when the transmission power is constrained. It can

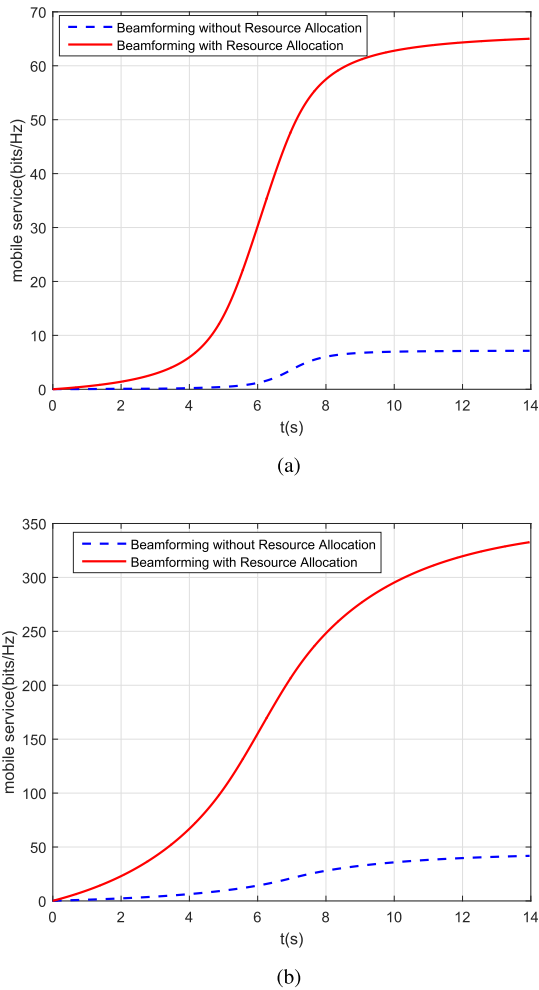


FIGURE 12. Mobile service comparison under different transmit power with/without resource allocation, $d_0 = 50$ m. (a) 30dBm. (b) 40dBm.

substantially improve the mobile service of one BS in this scenario and this tiny performance gap is aroused from the complexity-performance tradeoff of STBC-ABF, which is quite suitable for the HSR scenario since the adaptive beamforming can be hardly performed.

To further exhibit the performance degradation aroused by the inaccuracy of location information, we present the cumulative mobile service under diverse location information accuracies as in Fig. 10. The performance deterioration under large location information error is obvious. However, if a wireless system aided with an acceptable positioning system, i.e. the location information error is less than 6 m, a good beamforming performance can be guaranteed.

C. MULTIPLE CARRIAGE MOBILE SERVICE WITHOUT CONSIDERING INTERFERENCE

Besides, we consider the whole train mobile service improvement which we name it as cumulative mobile service. In Fig. 11, a cumulative mobile service comparison under diverse transmit power is exhibited since it stands for the overall service competence of one BS, which in fact, is the maximum data volume that can be transmitted during the

train traversing time. A significant performance improvement can be achieved by adopting STBC-LBF scheme in this HSR scenario and it is noticed that the improvement is much obvious when the transmit power is lower, where equal power allocation policy is adopted for beamforming.

Furthermore, as shown in Fig. 12, the cumulative mobile service with different resource allocation schemes are illustrated, where beamforming without resource allocation stands for equal transmit power allocation for each selected beam. The simulation results indicate that even when the instant CSI is not available, location-aware resource allocation for each beam is crucial for better performance because large-scale fading is dominant in this scenario and the location information is known. Besides, the whole resource allocation process can be also pre-calculated as the beamforming weight, which reduces the system complexity as well.

D. MULTIPLE CARRIAGE MOBILE SERVICE CONSIDERING INTERFERENCE

In addition, in multiple carriage occasion, Fig. 13 shows that if multiple beams are selected, inter-beam interference elimination is paramount in the beamforming application process, where this improvement will be much obvious when two trains encounter. By applying a location-aided interference elimination method, this performance degradation is eliminated.

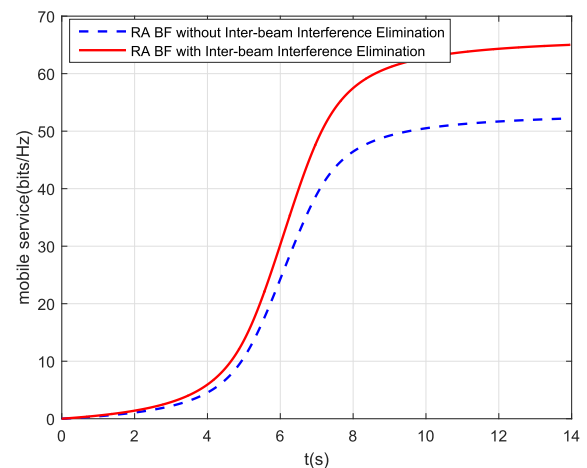


FIGURE 13. Mobile service comparison with/without inter-beam interference elimination, $d_0 = 50$ m.

VII. CONCLUSIONS

In this paper, aiming to solve the critical problems in the high mobility scenario, we presented a simple beamforming scheme with transmit diversity for massive MIMO systems which is practical and inexpensive to implement in the HSR scenario. Unlike traditional beamforming schemes, it needs neither transmit CSI nor UCCM and DCCM, which substantially decreases the system complexity with the help of train location information and therefore, it is applicable to either TDD systems or FDD systems. The whole beamforming process within one BS mainly depends on the location

information and the beamforming weight is also optimized according to this easy-to-get side information.

The diversity gain in this joint scheme is guaranteed with a simple optimal beam selection algorithm and a closed-form solution to maximize the multi-user mobile service is derived. When massive MIMO is applied in this scenario, the potential inter-beam interference is eliminated by a location-aided method. The simulation results indicate that our proposed beamforming with transmit diversity possesses a favourable performance with acceptable system complexity, which is suitable for the high mobility scenario.

APPENDIX A

Since total power \bar{P} at certain time is limited and the power allocation scheme at time t and time $t + 1$ is independent, to maximize the mobile service is equivalent to maximize the achievable rate $R(t)$ over the whole time period, namely,

$$\max_{f_n(t)} S^f \equiv \int_0^{t_m} \left[\max_{f_n(t)} R(\tau) \right] d\tau. \quad (35)$$

Therefore, the optimization problem is transformed as

$$\begin{aligned} & \max_{f_n(t)} R^f \\ & s.t. \quad \sum_{n=1}^N f_n(t) = 1, f_n(t) > 0. \end{aligned} \quad (36)$$

We set $P_n(t) = \bar{P} \cdot f_n(t)$ which represents the power allocated to beam n at time t and $\mathcal{W}(t) = h^2(t)/(\sigma_0^2 \cdot \sqrt{d^\alpha(t)})$.

Considering the Lagrangian function

$$\begin{aligned} F_w(t) = & \sum_{n=1}^{N_s} \log(1 + P_n(t) \cdot D_n(t) \cdot \mathcal{W}(t)) \\ & - \lambda \left(\sum_{n=1}^{N_s} P_n(t) - \bar{P} \right) - \sum_{n=1}^{N_s} \kappa_n P_n(t) / \bar{P}. \end{aligned} \quad (37)$$

With the Karush-Kuhn-Tucker (KKT) conditions, we have that $\kappa_n f_n(t) = 0$. According to the constraints in (25), $f_{k,n}(t)$ is positive. Hence, we have $\kappa_k = 0$ ($k = 1, \dots, K$). Then, based on Euler's formula, performing derivative of this integrand is equivalent to performing the derivative of $F_w(t)$. Therefore

$$\frac{\partial F_w(t)}{\partial P_n(t)} = \frac{D_n(t) \cdot \mathcal{W}(t)}{1 + P_n(t) \cdot D_n(t) \cdot \mathcal{W}(t)} - \lambda - \kappa_n / \bar{P}. \quad (38)$$

Setting $\partial L_w / \partial P_n = 0$, we get

$$P_n = \frac{1}{\lambda} - \frac{1}{D_n(t) \cdot \mathcal{W}(t)}. \quad (39)$$

Since the small-scale fading $h(t)$ is not known when the beamforming matrix is pre-set at the BS and large-scale fading $G(t)$ is dominant in this LOS scenario, we assume that $h(t)$ is a constant as in [49], namely $h(t) = 1$. Therefore, $\tilde{\mathcal{W}}(\tau) = 1/(\sigma_0^2 \cdot \sqrt{d^\alpha(\tau)})$ and the optimized power allocation coefficient

$$f_n(t) = \frac{1}{\lambda \bar{P}} - \frac{1}{\bar{P} \cdot D_n(t) \cdot \tilde{\mathcal{W}}(t)}. \quad (40)$$

The achievable rate $R(\tau)$ is monotonically increase when the train moves toward the BS and monotonically decrease when the train leaves the BS. It is possible that $f_n(t) = 0$ for $\tau \in [t, T]$ or $\tau \in [0, t]$. Therefore, our final goal is to obtain $f_n(t)$ after solving λ .

To find this λ , we utilize the power allocation coefficient constrain that $\sum_{n=1}^{N_s} f_n(t) = 1$. Then we have

$$\sum_{n=1}^{N_s} \left[\frac{1}{\lambda \bar{P}} - \frac{1}{\bar{P} D_n(t) \tilde{\mathcal{W}}(t)} \right] = 1. \quad (41)$$

By solving this equation, one can eventually obtain

$$\lambda = \frac{N_s}{\bar{P} + \sum_{n=1}^{N_s} \frac{1}{D_n(t) \tilde{\mathcal{W}}(t)}}. \quad (42)$$

By substituting λ into Eq. 18 and considering the fact that $f_{k,n}(t) \geq 0$, we obtain the closed-form of $f_n(t)$.

This completes the proof of **Proposition 1**.

APPENDIX B

The problem shown in (25) is a typical convex optimization with inequality constraints. Thus, by using the KKT conditions, we have following Lagrangian first

$$\begin{aligned} F_w = & \int_0^{t_s} \left[\sum_{k=1}^K R_k(\tau) \right] d\tau - \lambda \left(\int_0^{t_s} \sum_{k=1}^K \sum_{n=1}^N p_{k,n}(\tau) d\tau - \bar{P} t_s \right) \\ & - \int_0^{t_s} \sum_{k=1}^K \kappa_k p_{k,n}(\tau) d\tau \\ = & \int_0^{t_s} \left[\sum_{k=1}^K R_k(\tau) - \lambda \left(\sum_{k=1}^K \sum_{n=1}^N p_{k,n}(\tau) - \bar{P} \right) \right. \\ & \left. - \sum_{k=1}^K \kappa_k p_{k,n}(\tau) \right] d\tau \\ \triangleq & \int_0^{t_s} L_w(\tau) d\tau \end{aligned}$$

where $L_w(\tau) = \sum_{k=1}^K R_k(\tau) - \lambda \left(\sum_{k=1}^K \sum_{n=1}^N p_{k,n}(\tau) - \bar{P} \right) - \sum_{k=1}^K \kappa_k p_{k,n}(\tau)$. Since Large-scale fading is dominant in this scenario, we assume $h(t) = 1$ [49] and set $\mathcal{W}_k(t) = G_k^2(t)/\sigma_0^2$. Based on Euler's formula, performing derivative of this integrand is equivalent to performing the derivative of $F_w(t)$. Therefore,

$$\begin{aligned} \frac{\partial L_w(t)}{\partial p_{k,n}(t)} = & \frac{\sum_{n=1}^N i_{k,n} \cdot D_n(t) \cdot \mathcal{W}_k(t)}{1 + \sum_{n=1}^N i_{k,n} \cdot p_{k,n}(t) \cdot D_n(t) \cdot \mathcal{W}_k(t)} \\ & - \left(\lambda + \sum_{k=1}^K \kappa_k \right) K. \end{aligned}$$

Then, with the KKT conditions, we have that $\kappa_k f_{k,n}(t) = 0$. Because according to the constraints in (25),

$f_{k,n}(t)$ is positive, we have $\kappa_k = 0$ ($k = 1, \dots, K$). Setting $\partial L_w(t)/\partial p_{k,n}(t) = 0$, we can immediately get

$$p_{k,n}(t) = \frac{1}{\lambda K} - \frac{1}{\sum_{n=1}^N i_{k,n} \cdot D_n(t) \cdot \mathcal{W}_k(t)}.$$

Then the optimal power allocation coefficient is

$$f_{k,n}(t) = \frac{1}{\lambda K \bar{P}} - \frac{1}{\bar{P} \sum_{n=1}^N i_{k,n} \cdot D_n(t) \cdot \mathcal{W}_k(t)}.$$

To find this λ , we utilize the power allocation coefficient constrain that $\sum_{k=1}^K \sum_{n=1}^N f_{k,n}(t) = 1$. Then we have

$$\sum_{n=1}^N \left[\frac{1}{\lambda K \bar{P}} - \frac{1}{\bar{P} \sum_{n=1}^N i_{k,n} \cdot D_n(t) \cdot \mathcal{W}_k(t)} \right] = 1.$$

By solving this equation, one can eventually obtain

$$\lambda = \frac{1}{\bar{P} + \sum_{k=1}^K \frac{1}{\sum_{n=1}^N i_{k,n} \cdot D_n(t) \cdot \mathcal{W}_k(t)}}.$$

Considering the fact that $f_{k,n}(t) \geq 0$, (27) can be derived. This completes the proof of **Proposition 2**.

REFERENCES

- [1] I. F. Akyildiz, D. M. Gutierrez-Estevez, and E. C. Reyes, "The evolution to 4G cellular systems: LTE-Advanced," *Phys. Commun.*, vol. 3, no. 4, pp. 217–244, Dec. 2010.
- [2] J. Liu and E. Gunawan, "Combining ideal beamforming and Alamouti space-time block codes," *Electron. Lett.*, vol. 39, no. 17, pp. 1258–1259, Aug. 2003.
- [3] G. Jongren, M. Skoglund, and B. Ottersten, "Combining beamforming and orthogonal space-time block coding," *IEEE Trans. Inf. Theory*, vol. 48, no. 3, pp. 611–627, Mar. 2002.
- [4] L. Zhang, Y. Li, and L. J. Cimini, "Statistical performance analysis for MIMO beamforming and STBC when co-channel interferers use arbitrary MIMO modes," *IEEE Trans. Commun.*, vol. 60, no. 10, pp. 2926–2937, Oct. 2012.
- [5] L. Liu et al., "Position-based modeling for wireless channel on high-speed railway under a viaduct at 2.35 GHz," *IEEE J. Sel. Areas Commun.*, vol. 30, no. 4, pp. 834–845, May 2012.
- [6] J. Wang, H. Zhu, and N. J. Gomes, "Distributed antenna systems for mobile communications in high speed trains," *IEEE J. Sel. Areas Commun.*, vol. 30, no. 4, pp. 675–683, May 2012.
- [7] G. Barbu, "E-Train—Broadband communication with moving trains," Int. Union Railways (UIC), Chicago, IL, USA, Tech. Rep. 190_14, 2010.
- [8] B. Chow, M.-L. Yee, M. Sauer, A. Ng'oma, M.-C. Tseng, and C.-H. Yeh, "Radio-over-fiber distributed antenna system for WiMAX bullet train field trial," in *Proc. IEEE Mobile WiMAX Symp.*, Napa Valley, CA, USA, 2009, pp. 98–101.
- [9] W. Li et al., "Analytical model and performance evaluation of long-term evolution for vehicle safety services," *IEEE Trans. Veh. Technol.*, vol. 66, no. 3, pp. 1926–1939, Mar. 2017.
- [10] X. Chen, J. Lu, and P. Fan, "General hardware framework of Nakagami m parameter estimator for wireless fading channel," in *Proc. IEEE HMWC*, Xi'an, China, Oct. 2015, pp. 1–5.
- [11] O. Karimi, J. Liu, and C. Wang, "Seamless wireless connectivity for multimedia services in high speed trains," *IEEE J. Sel. Areas Commun.*, vol. 30, no. 4, pp. 729–739, May 2012.
- [12] C. Zhang, P. Fan, K. Xiong, and P. Fan, "Optimal power allocation with delay constraint for signal transmission from a moving train to base stations in high-speed railway scenarios," *IEEE Trans. Veh. Technol.*, vol. 64, no. 12, pp. 5775–5788, Dec. 2015.
- [13] Y. Cui and X. Fang, "Performance analysis of massive spatial modulation MIMO in high-speed railway," *IEEE Trans. Veh. Technol.*, vol. 65, no. 11, pp. 8925–8932, Nov. 2016, doi: 10.1109/TVT.2016.2518710.
- [14] B. Ai et al., "Challenges toward wireless communications for high-speed railway," *IEEE Trans. Intell. Transp. Syst.*, vol. 15, no. 5, pp. 2143–2158, Oct. 2014.
- [15] Y. Yang, P. Fan, and Y. Huang, "Doppler frequency offsets estimation and diversity reception scheme of high speed railway with multiple antennas on separated carriages," in *Proc. IEEE Wireless Commun. Signal Process. (WCSP)*, Huangshan, China, Oct. 2012, pp. 1–6.
- [16] Z. Lei, F. P. S. Chin, and Y.-C. Liang, "Orthogonal switched beams for downlink diversity transmission," *IEEE Trans. Antennas Propag.*, vol. 53, no. 7, pp. 2169–2177, Jul. 2005.
- [17] L. Tian, J. Li, Y. Huang, J. Shi, and J. Zhou, "Seamless dual-link handover scheme in broadband wireless communication systems for high-speed rail," *IEEE J. Sel. Areas Commun.*, vol. 30, no. 4, pp. 708–718, May 2012.
- [18] X. Chen, S. Liu, and P. Fan, "Position-based diversity and multiplexing analysis for high speed railway communications," in *Proc. IEEE HMWC*, Xi'an, China, Oct. 2015, pp. 41–45.
- [19] Y. Dong, P. Fan, and K. B. Letaief, "High-speed railway wireless communications: Efficiency versus fairness," *IEEE Trans. Veh. Technol.*, vol. 63, no. 2, pp. 925–930, Sep. 2014.
- [20] R. He, Z. Zhong, B. Ai, G. Wang, J. Ding, and A. F. Molisch, "Measurements and analysis of propagation channels in high-speed railway viaducts," *IEEE Trans. Wireless Commun.*, vol. 12, no. 2, pp. 794–805, Feb. 2013.
- [21] Y. Feng, R. Xu, and Z. Zhong, "Channel estimation and ICI cancellation for LTE downlink in high-speed railway environment," in *Proc. IEEE 11th Int. Conf. Signal Process. (ICSP)*, vol. 2, Oct. 2012, pp. 1419–1423.
- [22] X. Chen, J. Lu, S. Liu, and P. Fan, "Location-aided umbrella-shaped massive MIMO beamforming scheme with transmit diversity for high speed railway communications," in *Proc. IEEE VTC-Spring*, Nanjing, China, May 2016, pp. 1–5.
- [23] X. Ren, W. Chen, and M. Tao, "Position-based compressed channel estimation and pilot design for high-mobility OFDM systems," *IEEE Trans. Veh. Technol.*, vol. 64, no. 5, pp. 1918–1929, May 2015.
- [24] M. Médard, "The effect upon channel capacity in wireless communications of perfect and imperfect knowledge of the channel," *IEEE Trans. Inf. Theory*, vol. 46, no. 3, pp. 933–946, May 2000.
- [25] D. Tian, J. Zhou, Z. Sheng, and V. C. M. Leung, "Robust energy-efficient mimo transmission for cognitive vehicular networks," *IEEE Trans. Veh. Technol.*, vol. 65, no. 6, pp. 3845–3859, May 2016.
- [26] G. Baldini et al., "An early warning system for detecting GSM-R wireless interference in the high-speed railway infrastructure," *Int. J. Critical Infrastruct. Protection*, vol. 3, no. 3, pp. 140–156, Dec. 2010.
- [27] C. Zhang and P. Fan, "Providing services for the high-speed train and local users in the same OFDMA system: Resource allocation in the downlink," *IEEE Trans. Wireless Commun.*, vol. 15, no. 2, pp. 1018–1030, Feb. 2016.
- [28] H. Ghazzai, T. Bouchoucha, A. Alsharoua, E. Yaacoub, M.-S. Alouini, and T. Y. Al-Naffouri, "Transmit power minimization and base station planning for high-speed trains with multiple moving relays in OFDMA systems," *IEEE Trans. Wireless Commun.*, vol. 66, no. 1, pp. 175–187, Jan. 2016, doi: 10.1109/TVT.2016.2542344.
- [29] Z. Lei, F. Chin, and Y.-C. Liang, "Combined beamforming with spacetime block coding for wireless downlink transmission," in *Proc. IEEE VTC*, Sep. 2002, pp. 2145–2148.
- [30] M. Lin, M. Li, L. Yang, and X. You, "Adaptive transmit beamforming with space-time block coding for correlated MIMO fading channels," in *Proc. IEEE ICC*, Glasgow, Scotland, Jun. 2007, pp. 5879–5884.
- [31] Y. Ko, Q. Ma, and C. Tepedelenlioglu, "Comparison of adaptive beamforming and orthogonal STBC with outdated feedback," *IEEE Trans. Wireless Commun.*, vol. 6, no. 1, pp. 20–25, Jan. 2007.
- [32] H.-S. Cho, J. H. Chung, and D. K. Sung, "Four-sector cross-shaped urban microcellular systems with intelligent switched-beam antennas," *IEEE Trans. Veh. Technol.*, vol. 50, no. 2, pp. 592–604, Mar. 2001.
- [33] B. Allen and M. Beach, "On the analysis of switched-beam antennas for the W-CDMA downlink," *IEEE Trans. Veh. Technol.*, vol. 53, no. 3, pp. 569–578, May 2004.
- [34] M. I. Lai, T. Y. Wu, J. C. Hsieh, C. H. Wang, and S. K. Jeng, "Compact switched-beam antenna employing a four-element slot antenna array for digital home applications," *IEEE Trans. Antennas Propag.*, vol. 56, no. 9, pp. 2929–2936, Sep. 2008.
- [35] H. Wang, Z. Zhang, Y. Li, and M. F. Iskander, "A switched beam antenna with shaped radiation pattern and interleaving array architecture," *IEEE Trans. Antennas Propag.*, vol. 63, no. 7, pp. 2914–2921, Jul. 2015.
- [36] L. Yang, G. Ren, W. Zhai, and Z. Qiu, "Beamforming based receiver scheme for DVB-T2 system in high speed train environment," *IEEE Trans. Broadcast.*, vol. 59, no. 1, pp. 146–154, Mar. 2013.
- [37] B. Chen, Z. Zhong, B. Ai, and X. Chen, "Comparison of antenna arrays for MIMO system in high speed mobile scenarios," in *Proc. IEEE VTC-Spring*, Yokohama, Japan, May 2011, pp. 1–5.

- [38] M. Cheng, X. Fang, and W. Luo, "Beamforming and positioning-assisted handover scheme for long-term evolution system in high-speed railway," *IET Commun.*, vol. 6, no. 15, pp. 2335–2340, Oct. 2012.
- [39] W. C. Y. Lee, "An optimum solution of the switching beam antenna system," in *Proc. IEEE VTC*, Phoenix, AZ, USA, May 1997, pp. 170–172.
- [40] X. Chen and P. Fan, "Low-complexity location-aware multi-user massive MIMO beamforming for high speed train communications," in *Proc. IEEE VTC-Spring*, Sydney, NSW, Australia, Jun. 2017, pp. 1–6.
- [41] J. Lu, X. Chen, S. Liu, and P. Fan, "Location-aware low complexity ICI reduction in OFDM downlinks for high-speed railway communication systems with distributed antennas," in *Proc. IEEE VTC-Spring*, Nanjing, China, May 2016, pp. 1–5.
- [42] A. Goldsmith, *Wireless Communications*. Cambridge, U.K.: Cambridge Univ. Press, 2005.
- [43] H. Suzuki, "A statistical model for urban radio propagation," *IEEE Trans. Commun.*, vol. 25, no. 7, pp. 673–679, Jul. 1977.
- [44] X. Chen, S. Liu, J. Lu, P. Fan, and K. B. Letaief, "Smart channel sounder for 5G IoT: From wireless big data to active communication," *IEEE Access*, vol. 4, pp. 8888–8899, 2016, doi: [10.1109/ACCESS.2016.2628820](https://doi.org/10.1109/ACCESS.2016.2628820).
- [45] A. C. Balanis, *Antenna Theory: Analysis and Design*. Hoboken, NJ, USA: Wiley, 2005.
- [46] D. Tse and P. Viswanath, *Fundamentals of Wireless Communication*. Cambridge, U.K.: Cambridge Univ. Press, 2005.
- [47] W. Luo, X. Fang, M. Cheng, and Y. Zhao, "Efficient multiple group multiple antenna (MGMA) scheme for high speed railway viaduct," *IEEE Trans. Veh. Technol.*, vol. 62, no. 6, pp. 2558–2569, Jul. 2013.
- [48] S. Alamouti, "A simple transmit diversity technique for wireless communications," *IEEE J. Sel. Areas Commun.*, vol. 16, no. 8, pp. 1451–1458, Oct. 1998.
- [49] T. Li, Z. Chen, P. Fan, and K. Ben Letaief, "Position-based power allocation for uplink HSRs wireless communication when two trains encounter," in *Proc. IEEE GLOBECOM*, Washington, DC, USA, Dec. 2016, pp. 1–6.



XUHONG CHEN received the B.S. and M.S. degrees from the Department of Communication Engineering, Chongqing University, Chongqing, China, in 2010 and 2013, respectively. He is currently pursuing the Ph.D. degree in electronic engineering with Tsinghua University, Beijing, China. His research interests include high mobility broadband wireless communications, channel estimation, cross-layer design, and network information theory.



JIAXUN LU received the B.S. degree from Tsinghua University, Beijing, China, in 2014, where he is currently pursuing the Ph.D. degree in electronic engineering. His current research interests include high-speed railway wireless communications, with the emphasis on signal precoding and processing.



PINGYI FAN (M'03–SM'09) received the B.S. degree from the Department of Mathematics, Hebei University, in 1985, the M.S. degree from the Department of Mathematics, Nankai University, in 1990, and the Ph.D. degree from the Department of Electronic Engineering, Tsinghua University, Beijing, China, in 1994. From 1997 to 1998, he visited The Hong Kong University of Science and Technology as a Research Associate. From 1998 to 1999, he visited the University of

Delaware, USA, as a Research Fellow. In 2005, he visited NICT of Japan as a Visiting Professor. From 2005 to 2011, he visited The Hong Kong University of Science and Technology for many times and in 2011, he was a Visiting Professor with the Institute of Network Coding, The Chinese University of Hong Kong. He is currently a Professor with the Department of EE, Tsinghua University.

Dr. Fan is an Oversea Member of IEICE. He has attended to organize many international conferences, including as the General Co-Chair of the IEEE VTS HMWC2014, the TPC Co-Chair of the IEEE International Conference on Wireless Communications, Networking and Information Security (WCNIS 2010), and the TPC Member of the IEEE ICC, Globecom, WCNC, VTC, and Inforcom. He has served as an Editor of the IEEE TRANSACTIONS ON WIRELESS COMMUNICATIONS, the *International Journal of Ad Hoc and Ubiquitous Computing* (Inderscience), and the *Wiley Journal of Wireless Communication and Mobile Computing*. He is also a reviewer of more than 32 international journals, including 18 IEEE journals and 8 EURASIP journals. He has received some academic awards, including the IEEE Globecom 2014 Best Paper Award, the IEEE WCNC'08 Best Paper Award, the ACM IWCMC'10 Best Paper Award, and IEEE ComSoc Excellent Editor Award for the IEEE TRANSACTIONS ON WIRELESS COMMUNICATIONS in 2009. His main research interests include 5G technology in wireless communications, such as massive MIMO and OFDMA, network coding, network information theory, and cross layer design.



KHALED BEN LETAIEF (S'85–M'86–SM'97–F'03) received the B.S. (Hons.), M.S., and Ph.D. degrees from Purdue University, West Lafayette, IN, USA, in 1984, 1986, and 1990, respectively, all in electrical engineering. In 1985, he was with the School of Electrical and Computer Engineering, College of Engineering, Purdue University, where he has taught courses in communications and electronics as a Graduate Instructor.

From 1990 to 1993, he was a Faculty Member with the University of Melbourne, Australia. Since 1993, he has been with The Hong Kong University of Science and Technology, where he is currently a Chair Professor and the Head of the Electronic and Computer Engineering Department. He is also the Director of the Hong Kong Telecom Institute of Information Technology. His current research interests include wireless and mobile networks, broadband wireless access, cooperative communications, cognitive radio, OFDM, CDMA, and beyond 3G systems. In these areas, he has authored over 300 journal and conference papers and given invited keynote talks as well as courses all over the world.

Dr. Letaief served as a consultant for different organizations and is the founding Editor-in-Chief of the IEEE TRANSACTIONS ON WIRELESS COMMUNICATIONS. He has served on the editorial board of other prestigious journals including the IEEE JOURNAL ON SELECTED AREAS IN COMMUNICATIONS—Wireless Series (as an Editor-in-Chief). He has been involved in organizing a number of major international conferences and events. These include serving as the Technical Program Chair of the 1998 IEEE Mini-Conference on Communications Theory, the Co-Chair of the 2001 IEEE Communications Theory Symposium, the Co-Chair of the 2004 IEEE Wireless Communications, Networks and Systems Symposium, and the Co-Technical Program Chair of the 2004 IEEE International Conference on Communications, Circuits and Systems. He is the General Chair of the 2007 IEEE Wireless Communications and Networking Conference; as well as the Technical Program Co-Chair of the 2008 IEEE International Conference on Communication. He served as the Chair of the IEEE Technical Committee on Personal Communications.

He is an IEEE Distinguished Lecturer of the IEEE Communications Society, and an elected member of the IEEE Communications Society Board of Governors.

...